OUKA
Osaka University Knowledge Archive

Title	Ion and Neutral Particle Diagnostics in Reactive ECR Plasma(Physics, Process, Instruments & Measurements)
Author(s)	Chen, Wei; Yoshinaga, Jun; Setsuhara, Yuichi; Miyake, Shoji
Citation	Transactions of JWRI. 20(2) P.203-P.209
Issue Date	1991-12
Text Version	publisher
URL	http://hdl.handle.net/11094/10653
DOI	
rights	本文データはCiNiiから複製したものである
Note	

Osaka University Knowledge Archive : OUKA

https://ir.library.osaka-u.ac.jp/repo/ouka/all/

Osaka University

Ion and Neutral Particle Diagnostics in Reactive ECR Plasma

Wei CHEN*, Jun YOSHINAGA, Yuichi SETSUHARA***and Shoji MIYAKE******

Abstract

High resolution optical measurements of Doppler profiles of Ar neutral lines have been performed to determination the average translational energies of Ar neutral in an electron cyclotron resonance (ECR) process plasma. Preliminary experiments Ar and Ar / H_2 mixture gases have been used in the operating pressure range of 10^{-2} to 3×10^{-1} Pa with microwave power (2.45 GHz) of 165-495 W. The optical emission line profiles from source plasma have been measured in parallel and perpendicular directions to the axis of magnetic coils, yielding the Ar energies of 0.9 eV in parallel geometry and 0.2 eV in perpendicular geometry. Also presented in this paper are measurements of the ion species distribution in Ar, H_2, N_2 and CH_4 / Ar mixture plasmas using a time-of-flight (TOF) analyzer. The TOF analysis in an H_2 plasma has shown that the main ion species are molecular ions of H_3^+ or H_2^+ in the typical operating pressure of $10^{-3}-10^{-1}$ Pa.

KEY WORDS : (ECR Process Plasma) (Fabry-Perot Interferometer) (Doppler Broadening) (Zeeman Broadening) (Time-Of-Flight TOF)

1. Introduction

Electron cyclotron resonance (ECR) plasmas are receiving considerable attention from the applications of plasma processing due to their high degree of ionization and high reactive species density, low and controllable plasma sheath potential and electrodeless operation[1-4]. These factors make the ECR process plasma attractive for ion beam technologies and high-rate single-wafer etching, deposition in highly reactive gases with reducing damage and contamination compared to competing radio-frequency (rf) discharges.

In spite of the successful application of ECR plasma in the material processes, information of ECR plasma property and its controllability on the ECR plasma has not been obtained yet enough to explain the mechanism of the processes. In a previous work, we have clarified that the spatial structure of ECR process plasmas in hydrogen gas[5], where the electron energy and its density in the plasma space indicated remarkably non-uniform distributions in both mirror and divergent magnetic fields, in a gas pressure range of several Pa to 10^{-2} Pa, inherent to the local feature of ECR phenomenon. The electron temperature and density were shown to be much higher value around the resonance region than those in the down stream. Appearance of these peaks were found to correspond well to the cyclotron damping of the input microwave near the resonance zone.[6] The propagation and damping of the microwave has shown that the plasma production is dominated by electron cyclotron absorption of the wave. While in our experiment of a-C:H and a-Si:H films synthesis[7-8], the highest deposition rate was obtained around the resonance region and also the film compositions were found to be different in space.

From these results we have demonstrated that studying the local effect of ECR phenomenon is a key problem in the optimum and high-quality film synthesis by ECR process plasmas.

Furthermore we have a great interest in the behaviors of neutrals and ions in the plasma, which are the direct reactive elements for plasma processes. In this paper we like to discuss tow topics. One is determination of ion temperature (T_i) and neutral temperature (T_n) based on the measurement of the Doppler broadening of the optical emission lines of ions and neutrals using a Fabry-Perot interferometer. The other is the measurement of the ions species distributions using a time-of-flight (TOF) analyzer.[10-12]

2. Experimental apparatus

2.1 Optical emission spectroscopy using Fabry-Perot

The ECR plasma source and the optical system used in

† Received on Nov,9,1991

* Graduate School Student of Osaka University
** Graduate School of Student Kansai University
*** Research Instructor
**** Professor

Transactions of JWRI is published by Welding Research Institute, Osaka University, Ibaraki, Osaka 567, Japan

the present work is schematically shown in **Fig. 1**, and ECR plasma source part is described in detail elsewhere[5] so that only those aspects relevant to the optical measurement system is described. Optical emission line profiles have been measured from two orientations, i.e. i) transverse to the axis of the plasma source in the midplane of the two coils (perpendicular view), and ii) along the axis viewing the plasma from the other end of the microwave entrance port (parallel view). The emission from the plasma was collected onto 50 cm monochromator operating as a pass-band filter to select the emission line. The light exiting the monochromator was coupled to an optical fiber, collimated and pass through a Fabry-Perot interferometer, and detected by a photomultiplier tube.

The instrumental response of this optical system was determined using a He-Ne laser beam (632.8 nm). **Figure 2** shows a typical profile of He-Ne laser light obtained by the optical system. The measured response presents a 0.0014 nm full width at half maximum (FWHM) intensity of Gaussian line profile, resulting in the system resolution of $\Delta \lambda_{\text{He-Ne}} / \lambda_{\text{He-Ne}} = 2 \times 10^{-6}$.

The Doppler width (FWHM) $\Delta \lambda_D$ was determined

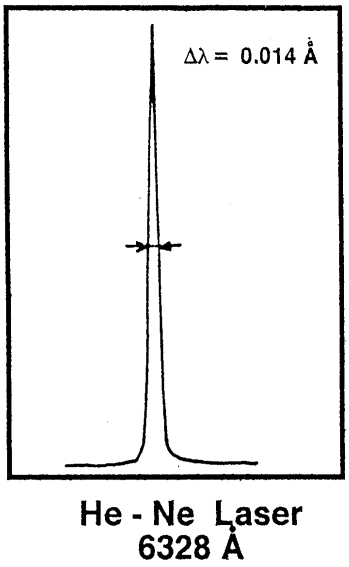

Fig. 2 Typical profile of He-Ne laser (632.8 nm) measured by Fabry-Perot interferometer.

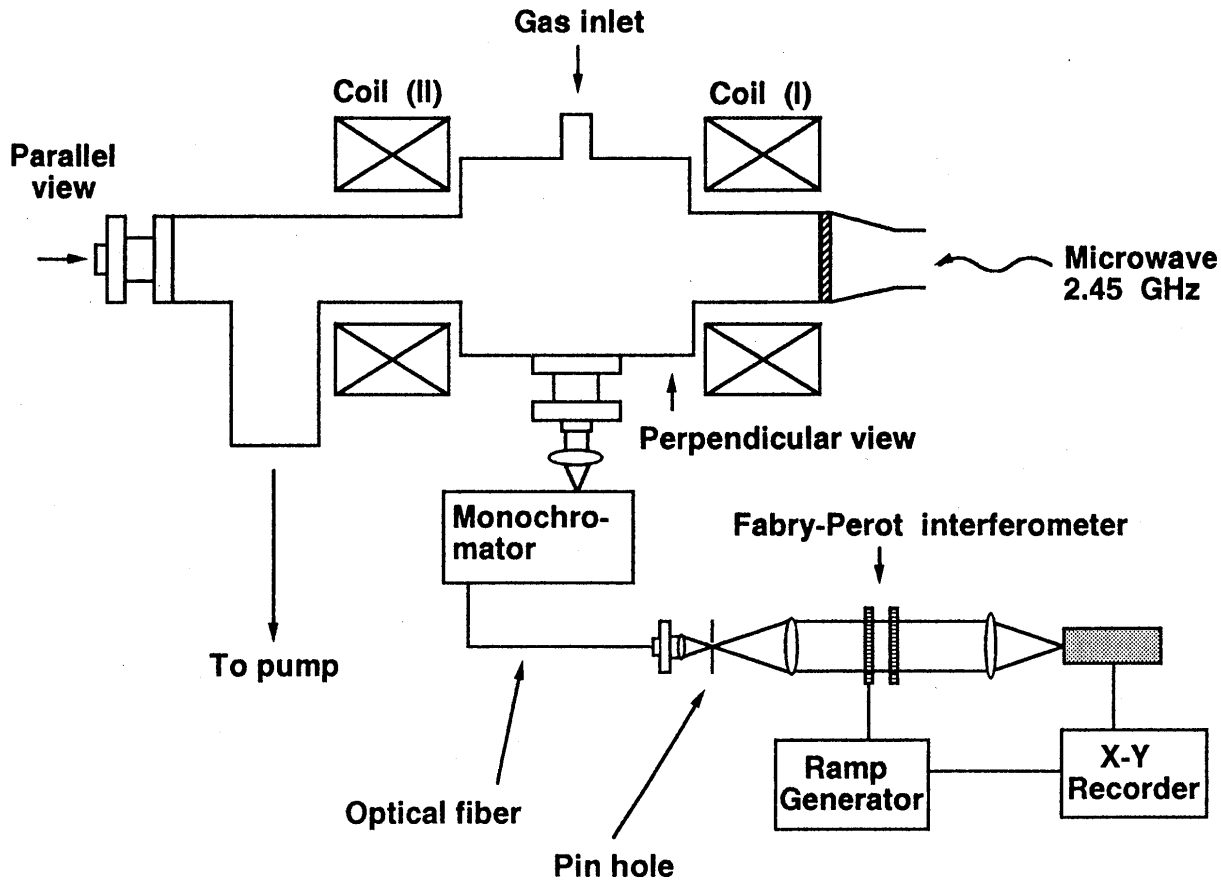

Fig. 1 Schematic diagram of high resolution optical system alignment.

from the measured spectral line width (FWHM) $\Delta\lambda_{meas}$ by the following equation

$$(\Delta\lambda_D/\lambda)^2 = (\Delta\lambda_{meas}/\lambda)^2 - (\Delta\lambda_{He\text{-}Ne}/\lambda_{He\text{-}Ne})^2 \quad (1)$$

since the Ar spectral lines shapes measured for temperature determination appeared to have Gaussian profile (see section 3.1). Thus the temperature of emitting species with a mass A can be given by

$$T = 1.68 \times 10^{-8} A (\Delta\lambda_D/\lambda)^2 \quad (2)$$

where T is in eV and A is in amu.

As a preliminary study of ECR process plasma, argon and argon / hydrogen (1 : 1) mixture discharges are used in this work. Emission line profiles were measured as a function of microwave power (165-495 W), and gas pressure ($10^{-2} - 3 \times 10^{-1}$ Pa) in a divergent magnetic field.

2.2 TOF ion species analyzer system

A schematic diagram of the TOF system is presented in **Fig. 3** (a). The TOF analyzer consisted of four sections: 1) the accelerating / focusing lens, 2) the deflection plates, 3) the time-of-flight length and 4) the ion detector. Figure 3 (b) shows the first two sections. If potential is measured relative to the plasma, then the entrance aperture is

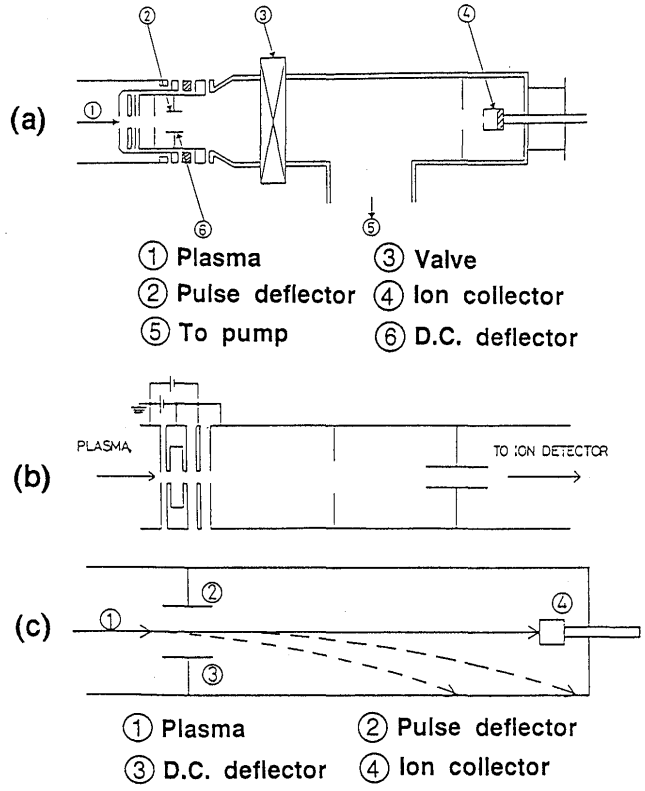

Fig. 3 Schematic diagram TOF analyzer included accelerating/focusing lens, collimator and deflection plates.

negative by the plasma potential (V_p). The second aperture is biased at a high negative voltage (V_b) to accelerate the ions to 2-3kV. It is important that this bias voltage be much greater than the ion temperature, otherwise the TOF will depend more on temperature than on $(m_i/q_i)^{1/2}$. These two accelerating apertures make up a convergent lens with a focal length approximately equal to three times the distance between them. Thus after several centimeters the ion beam becomes strongly unfocused and the ion density starts to decline. An einzel lens is therefore placed after the accelerating lens in order to refocus the beam and thus increase the amount of current reaching the ion detector. The einzel lens does not change the ion's energy because the entrance and exit apertures are at the same potential.

After leaving the accelerating and focusing lens the ion beam is collimated and passes between two electrostatic deflection plates. Normally one plate is biased relative to the other, creating an electric field which deflects the ions. Figure 3 (c) shows the trace of ion beam extracted from plasma and passing through the deflectors to reach the detector. One of the deflection plate was biased at a constant negative voltage of several hundreds volts to inhibit the extracted ion beam from reaching the detector in the absence of the negative pulse biased on the other plate, in order to send a burst of ions to the detector only during the pulse duration. Thus the time required for the ions to transfer the detector is given by

$$\Delta t = L (m_i/zg_iV_b)^{1/2} \quad (3)$$

where L is the distance between the deflector and the detector, and V_b is accelerating bias voltage, m_i and q_i are the mass and the charge of the ion, respectively.

A simple Faraday cup was used to collect the ion current and the data acquisition was performed using an oscilloscope (Tektronix 2432A, Sony).

3. Results and discussion

3.1 Determination of ion and neutral kinetic energy in the ECR process plasma

In this study, neutral Ar emission lines of 811.5 nm (4p $[5/2]_3$-4s $[3/2]_2$) transition), 750.4 nm (4p' $[1/2]_0$-4s' $[1/2]_1$ transition) and Ar^+ emission line of 480.6 nm ($4p^4P^0_{5/2}$-$4s^4P_{5/2}$ transition) were applied to determinate the average translational energy of the particles in the ECR plasma. The emission line profiles were investigated before detailed studies on the effect of ECR plasma parameters. **Figure 4** shows the emission profile of neutral Ar in 4p $[5/2]_3$-4s $[3/2]_2$) and 4p' $[1/2]_0$-4s' $[1/2]_1$ transitions measured by using the high-resolution Fabry-Perot interferometer. The emission profiles of 815.5 nm

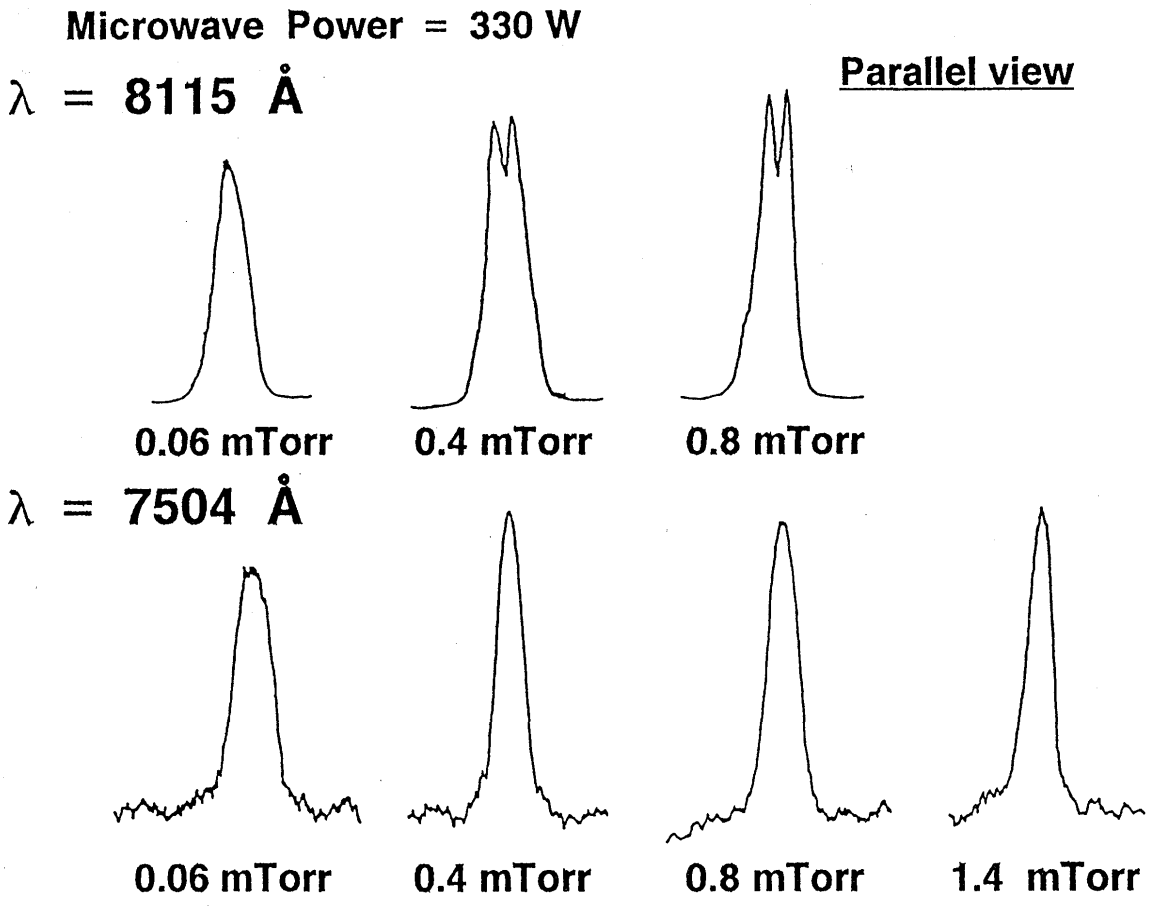

Fig. 4 Profiles of emission lines of 811.5 nm (4p $[5/2]_3$-4s $[3/2]_2$) transition), 750.4 nm (4p' $[1/2]_0$-4s' $[1/2]_1$ transition) of neutral Ar from ECR plasma at various gas pressure.

transition from the plasma show significant self-absorption with increasing gas pressure. This result indicates that ECR discharges are optically thick for this transition which is terminated on long-lived (metastable) energy levels. On the other hand transition of 4p' $[1/2]_0$-4s' $[1/2]_1$ 750.4 nm line shows little self-absorption even when the gas pressure was increased to 1.4 mTorr. These transition emission line profiles in various gas pressure were found to be symmetric and Gaussian in shape rather than Lorentzian. Thus this emission line (750.4 nm) is applied to determine the average translational energy of Ar neutral.

The average energies of neutral Ar in Ar and Ar/H_2 plasma as function of gas pressure with various input microwave powers are shown in **Fig. 5** and **Fig. 6**, respectively. Both in the Ar and Ar/H_2 plasmas the neutral Ar energy is about 0.9 eV in parallel direction and 0.2 eV in perpendicular direction, where the line emission profile broadening is only considered as Doppler broadening. Actually, the line broadening depends on many factors, such as natural and collisional broadening, Zeeman broadening. In this experiment the first tow factors are insignificant compared to Doppler broadening. However in a magnetically confined ECR plasma the Zeeman splitting is an additional broadening included in measured profiles. The Zeeman broadening may be evaluated of the order $\Delta \lambda_{Zeeman} = 10^{-9} \lambda^2 B$, where wavelengths are in angstrom and magnetic field strengths is in kilogauss[9]. Thus as a result of the experiments the emission profiles observed in parallel and perpendicular views contains the Zeeman broadening less than 10% and 30%, respectively.

In the ECR plasma the electrons heated in the resonance zone and diffused out of ECR source by the gradient of magnetic field, resulting in an ambipolar potential which, in turn, accelerates ions in parallel direction of magnetic flux. Thus it can be predicted that $T_{i(parallel)} > T_{i(perpendicular)}$ in the ECR plasma. Meanwhile the neutral energy in the process plasma is determined by collisional transfer from all argon ion species so that the neutral energies exhibits significantly different quantities in the parallel and perpendicular directions as the data presented in Fig. 5 and Fig. 6. These data also show that $T_{n(parallel)}$ depends a little on the gas pressure due to

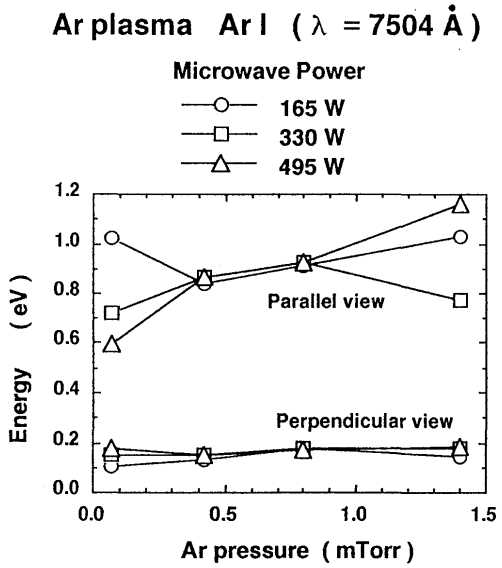

Fig. 5 Average neutral Ar energies vs. gas pressure with various microwave powers in Ar ECR plasma.

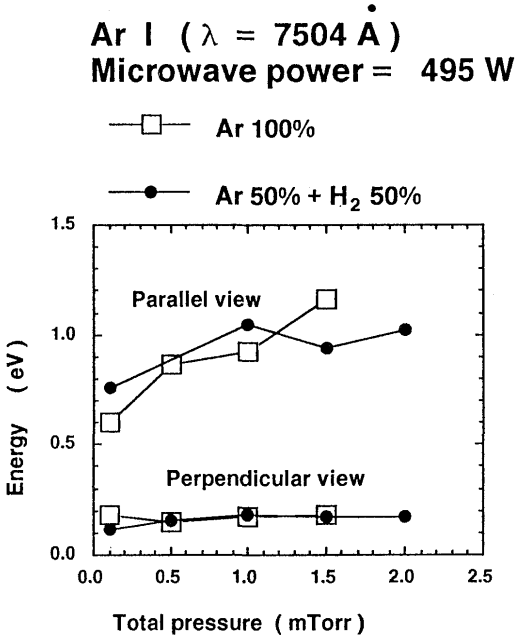

Fig. 6 Average neutral Ar energies vs. gas pressure in Ar and Ar / H_2 plasma.

increasing of the particle density; i.e. means more frequent ion-neutral collision occurred with increasing gas pressure. However, in the perpendicular direction $T_{n(perpendicular)}$ shows little change in the various gas pressure. The energy of Ar atom also exhibits little change on the microwave power and hydrogen gas mixture. The results obtained in our experiment correspond well to the result of John S. Mckillop et al[13].

The ion energies are predicted to be much higher than neutrals. In this preliminary study, however, the ion emission intensity drastically decreased after passing through the monochromator and thus it was difficult to get high signal-to-noise ratio in the current experiment.

3.2 Measurement of ion species by TOF analyzer

Typical TOF data is shown in **Fig. 7**, which obtained from Ar, N_2 and H_2 plasma, respectively. On the upper trace of each data the gate pulse of 200 ns duration to separate the ion species is shown. In the argon plasma singly and doubly ionized ions are observed. The second picture shows the N^+ and N_2^+ spectra from the N_2 plasma. In the hydrogen plasma, the third picture, we observed various molecular ions with H_3^+, H_2^+, as well as H^+ ions.

Figure 8 shows variation of N^+ and N_2^+ ion currents as the functions of gas pressure. It is interesting that in the pressure higher than 7×10^{-2} Pa the quantity of molecular ion is more than the quantity of atom ion.

A similar result obtained from hydrogen gas plasma is shown in **Fig. 9**. In this data it is important to find that H_3^+ ion is the main ion species in the gas pressure higher than 5×10^{-2} Pa in the H_2 plasma, and even in the region of 10^{-3} Pa H_2^+ still has the highest concentration. The result presented here also reflects the recombination process between ions and neutrals occurred frequently in gas pressure higher than 5×10^{-2} Pa. These data also gives that the resolvability of reactive molecular gas in ECR plasma.

We have demonstrated that the molecular ions are main ion species in the typical operating pressure of an ECR process plasma. The results presented here are also important for the determination of average mass of ions for the Langmuir probe measurement. Meanwhile H_2 gas is very frequently used as a dilution gas for plasma CVD, for example, in diamond, a-Si:H film synthesis and etc so that it can be predicted that the effect of the H_3^+, H_2^+ ions in the CVD surface reaction will become a negligibleless problem in the process of film deposition by an ECR plasma.

CH_4 admixed with Ar gases plasma also has been experimentally measured by TOF analyzer. **Figure 10** shows the mass spectra of the plasma with different microwave powers. As the main ion species in plasma H_1^+, H_2^+, H_3^+, CH_2^+, CH_3^+, C_2^+, $C_2H_2^+$ and Ar^+ is observed. In these data the vertical range is 500 μV in the microwave power of 330 W and 200 μV in the microwave power of 160 W, respectively. Increasing the microwave power the gases are furthermore dissociated/dissolved in the plasma, resulting the increasing of total ion current and changing of the ratio of the peak values of ion current as shown in **Fig. 10**. These spectra are also noticeable that the molecular ion is main ion species

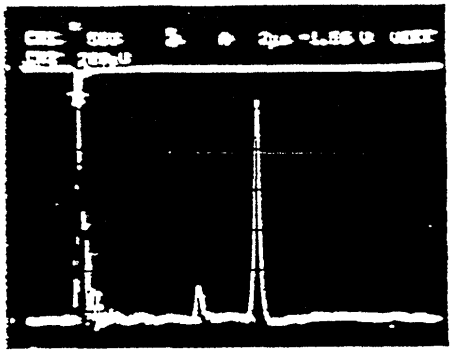

Ar Plasma $p_0 = 2.4 \times 10^{-1}$ Pa
P_μ =330 W τ_μ = 5 msec
V_b = -2.0 kV V_d = -250 V
Vp =-250 V τ_μ = 200 nsec

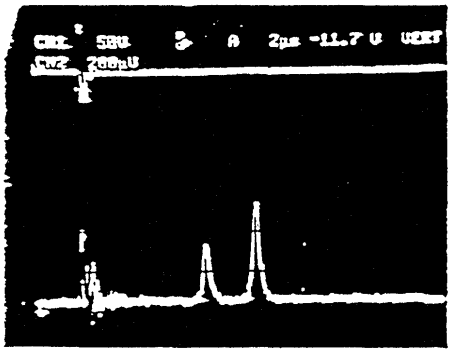

N_2 Plasma $p_0 = 2.4 \times 10^{-2}$ Pa
P_μ =330 W τ_μ = 5 msec
V_b = -2.0 kV V_d = -200 V
Vp =-200 V τ_μ =200 nsec

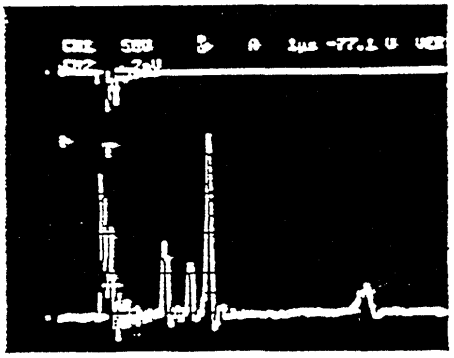

H_2 Plasma $p_0 = 3.0 \times 10^{-2}$ Pa
P_μ =330 W τ_μ = 5 msec
V_b = -2.0 kV V_d = -200 V
Vp =-200 V τ_μ = 200 nsec

Fig. 7 Typical ion species spectra obtained from Ar, N_2, H_2 plasma by applying TOF analyzer.

at the gas pressure of 5.8×10^{-2} Pa in the CH_4/Ar plasma. The gas pressure in this experiment was set in much lower value than a usual one for plasma CVD, thus it can predict that the molecular ions and/or even the large molecular ions exist and influence the CVD process, such as diamond film synthesis, where the gas pressure is normally set over several ten Pa.

4. Conclusion

Neutral Ar energy has been measured using high resolution Fabry-Perot interferometer at the gas pressure range of $1 \times 10^{-2} - 2 \times 10^{-1}$ Pa in the Ar and Ar/H_2 ECR plasmas. The energy of Ar is determined by collisional energy transfer from Ar^+ species in the plasma resulting in a large ratio of $T_{n(parallel)}$ to $T_{n(perpendicular)}$. The higher density of energetic ions and increased collision probability at higher gas pressure leads to observable increase in neutral energy in the parallel direction. The Ar neutral energy depends little on the input microwave power in the range of 160-500 W.

Various gases ECR plasmas have been measured by TOF analyzer. It was demonstrated that molecular ions are the main ion species in the reactive gas ECR plasma. This result indicates that the effect of the molecular ions is an important factor in the ECR plasma process.

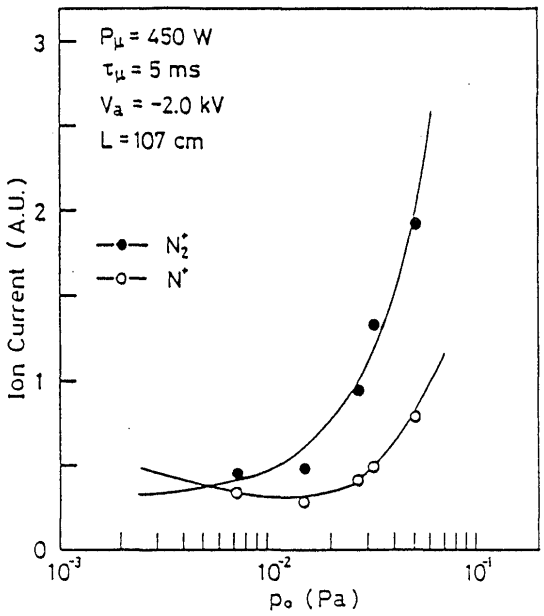

Fig. 8 Ion currents vs. gas pressure in N_2 plasma.

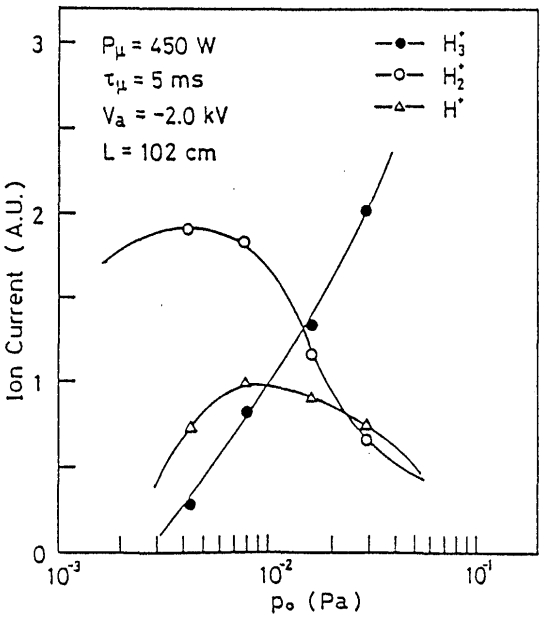

Fig. 9 Ion currents vs. gas pressure in H_2 plasma.

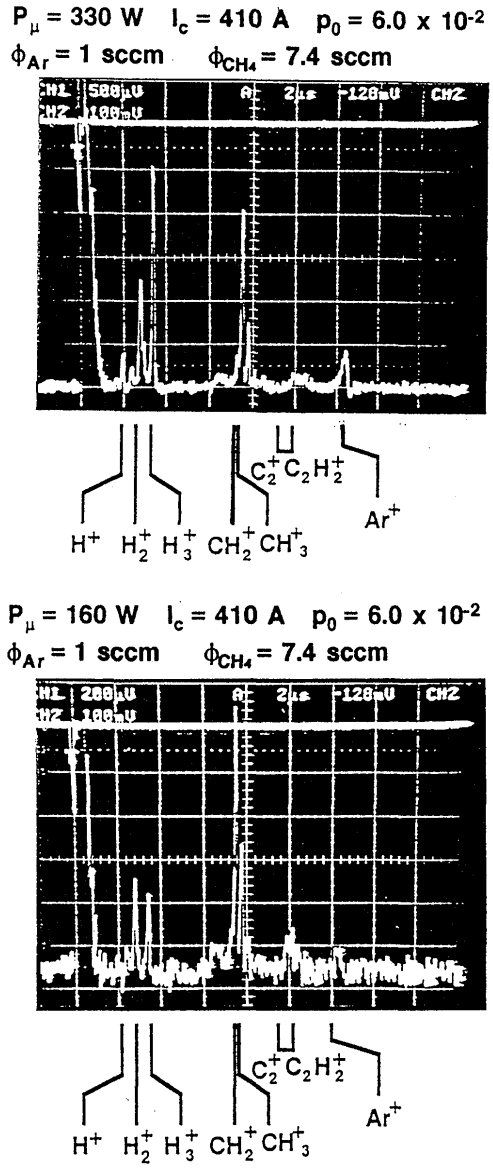

Fig. 10 Ion species spectra of CH_4/Ar plasma in different microwave powers.

References

1) M. Matsuoka and K. Ono, J. Vac. Sci. Technol. **A6(1)**, 25 (1982)
2) T. Ono, C. Takahasi, and S. Mastuo, Jpn. J. Appl. Phys. **23**, L534 (1984).
3) T. Ono, M. Oda, C. Takahasi, and S. Mastuo, J. Vac. Sci. Technol. **B4**, 696 (1986).
4) M. Shimada and Y. Torii, in Proceedings of the 10th Symposium on Ion Sources and Ion-Assisted Technology (ISIAT), Kyoto, 1986, p.471.
5) S. Miyake, W. Chen, and T. Ariyasu, Jpn. J. Appl. Phys. **29** 2491-2496 (1990).
6) W. Chen, S. Miyake, J. Yoshinaga and T. Ariyasu, in Proceedings of the International Seminar on Reactive Plasma, Nagoya, Japan, (1991), p.19.
7) S. Miyake, W. Chen, in Proc. 2nd.Int. Conf. on Plasma Surface Engineering, Garmisch-Partenkirchen F.R.G. Mat. Sci. Eng. A13a/1-2 (1991)294-301.
8) W. Chen, H. Takimoto and S. Miyake, in Proceedings of 8th Symposium on Plasma Processing, Nagoya, 1991, p.265.
9) H. R. Griem, Plasma spectroscopy, (McGraw-Hill, New York, 1964)
10) David Pinkston, Martin Rabb, J. Throck Watson and John Allison, Rev. Sci. Instr. **57**, 583 (1986).
11) Rathmann, N. Exeler and B. Willerding, J. Phys. E: Sci. Instrum. **18**, 17 (1985).
12) J. A. Browder, R. L. Miller, W. A. Thomas and G. Sanzone, Int. J. Mass Spectrosc. & Ion Phys. **37**, 99 (1981).
13) John S. Mckillop, John C. Forster, and William M. Holber, Appl. Phys. Lett. **55(1)**, 30-32 (1989).